where $\xi' = \phi$. Clearly, for every set of values $W(\xi')$, $Y(\xi')$ the relationship can be obtained for various Biot numbers.

The effectiveness factor can be obtained by either interpolating through successive $X$ vs. $\theta$ points and differentiating or by a simple averaging procedure:

$$\eta = \frac{(\nu + 1)[W(\xi', \theta_2) - W(\xi', \theta_1)]}{\xi'(\theta_2 - \theta_1)} = \frac{X(\theta_2) - X(\theta_1)}{\theta_2 - \theta_1} \tag{18}$$

Owing to the smoothness of the curves involved, it was found that interpolation is necessary only through three successive points and that Equation (18) provides an answer accurate at worst to two significant figures.

In this note we have shown how to find conversion and effectiveness factors efficiently from the SDRM when model parameters are known. Complete $X$ vs. $\theta$ and $\eta$ vs. $\theta$ plots can be formed at all values of $\phi$ and $Bi_m$ at very low costs which are several orders of magnitude lower than when a finite-difference scheme is employed. In addition, it has also been shown that solid- and gas-point concentrations can be determined by the integral transformation method (Dudukovic, 1975). The use of the method in problems of parameter identification and other applications will be described in the near future (Dudukovic and Lamba, 1976).

It has come to the author's attention that a similar transformation has in the meantime been independently discovered by Professor Bischoff, Cornell University, and his co-workers.


## ACKNOWLEDGMENT

The author is grateful to the National Science Foundation for financial support of the studies on gas solid noncatalytic reactions (Grant No. ENG76-00700).


## NOTATION

$Bi_m = k_m L/D_e$ = Biot number for mass transfer, dimensionless
$C_A$ = concentration of reactant $A$ in the pellet, moles cm$^{-3}$
$C_{A_o}$ = concentration of reactant $A$ in the bulk of the gas phase, moles cm$^{-3}$
$C_S$ = concentration of solid reactant S, moles cm$^{-3}$
$C_{S_o}$ = initial concentration of reactant S, moles cm$^{-3}$
$D_e$ = effective diffusivity of gaseous reactant $A$ through the pores of the solid pellet, cm$^2$ s$^{-1}$
$k$ = apparent rate constant, moles$^{-1}$ cm$^3$ s$^{-1}$
$k_d$ = deactivation rate constant, moles$^{-1}$ cm$^3$ s$^{-1}$
$k_m$ = mass transfer coefficient, cm s$^{-1}$
$L$ = characteristic dimension of solid pellets slab half thickness, radius of the cylinder or sphere, cm
$r = k_d/k$ = ratio of deactivation and main reaction rate constant assumed much less than one, dimensionless
$t$ = time, s
$W$ = dependent variable defined by Equation (14$a$), dimensionless
$X$ = conversion of the solid reactant S, dimensionless
$Y$ = cumulative gas reactant concentration as defined by Equation (8), dimensionless
$Y_o$ = cumulative gas reactant concentration in the center of the pellet, dimensionless
$y = C_A/C_{A_o}$ = gas reactant concentration, dimensionless
$Z$ = average solid reactant concentration as defined by Equation (5), dimensionless
$z = C_S/C_{S_o}$ = solid reactant concentration, dimensionless

### Greek Letters

$\alpha, \beta, \gamma, \delta$ = stoichiometric coefficients, dimensionless
$\epsilon$ = pellet porosity, dimensionless
$\eta$ = catalyst effectiveness factor, dimensionless
$\theta = k(\beta/\alpha)C_{A_o}t$ = time for gas solid noncatalytic reactions
$\theta = k_d(\beta/\alpha)C_{A_o}t$ = dimensionless time for parallel catalyst deactivation
$\xi = \xi_a/L$ = dimensionless space coordinate
$\xi_a$ = dimensional space coordinate, cm
$\xi'$ = dimensionless coordinate defined by Equation (9)
$\nu$ = parameter
$\phi = \left(\frac{kC_{S_o}}{D_e}\right)^{1/2} L$ = modulus for gas solid noncatalytic reaction, dimensionless
$\phi = \left(\frac{kC_{S_o}(1 + r)}{D_e}\right)^{1/2} L$ = modulus for parallel catalyst deactivation, dimensionless

## LITERATURE CITED


Dudukovic, M. P., "Analysis of Gas-Solid Noncatalytic or Catalyst Deactivation Reactions," paper presented at 68th Annual AIChE Meeting, Los Angeles, Calif. (Nov., 1975).

———, and H. Lamba, "Models for Gas Solid Reactions" (1976).

Khang, S. J., and O. Levenspiel, "The Suitability of nth-Order Rate Form to Represent Deactivating Catalyst Pellets," *Ind. Eng. Chem. Fundamentals*, **12**, No. 2, 185 (1973).

Lacey, D. T., J. H. Bowen, and K. S. Basden, "Theory of Noncatalytic Gas-Solid Reactions," *ibid.*, **4**, No. 3, 275 (1965).

Masamune, S., and J. M. Smith, "Performance of Fouled Catalyst Pellets," *AIChE J.*, **12**, No. 2, 384 (1966).

Murakami, Y., R. Kobayashi, T. Hattori, and M. Masuda, "Effect of Intraparticle Diffusion on Catalyst Fouling," *Ind. Eng. Chem. Fundamentals*, **7**, No. 4, 599 (1968).

Pigford, R. L., and G. Sliger, "Rate of Diffusion Controlled Reaction Between a Gas and a Porous Solid Sphere," *Ind. Eng. Chem. Process Design Develop.*, **12**, No. 1, 85 (1973).

Wen, C. Y., "Noncatalytic Heterogeneous Solid Fluid Reaction Models," *Ind. Eng. Chem.*, **60**, No. 9, 34 (1968).



*Manuscript received May 25, 1976; revision received June 21, and accepted June 22, 1976.*


# Vortex Inhibition: Velocity Profile Measurements


**C. S. CHIOU**
**and**
**R. J. GORDON**

**Department of Chemical Engineering**
**University of Florida**
**Gainesville, Florida 32611**


In 1971, we reported a new dilute polymer solution phenomenon termed vortex inhibition (VI) (Balakrishnan and Gordon, 1971; Gordon and Balakrishnan, 1972). VI refers to the disappearance of the air core or vortex which

ordinarily forms during the drainage of a liquid from a tank. It occurs following addition of minute quantities of various drag reducing polymers, with relative drag reducing ability correlating closely with the minimum polymer concentration for inhibition (denoted $C_{VI}$). Both $C_{VI}$ and drag reducing ability are highly sensitive to polymer degradation, and both also vary in the same fashion with changes in polymer conformation in solution (Gordon and Balakrishnan, 1972; Balakrishnan and Gordon, 1975*a*). Fundamental studies of VI are therefore of interest both in their own right and also because of the possibility that they may yield information on the mechanism of drag reduction.

Many investigators have suggested that the elongational viscosity of dilute polymer solutions plays a major role in the drag reduction phenomenon (Seyer and Metzner, 1969; Paterson and Abernathy, 1970; Little et al., 1975). Polymer solutions are known to exhibit exceptionally large elongational viscosities (Metzner and Metzner, 1970; Balakrishnan and Gordon, 1975*b*; Everage and Gordon, 1971), and since the flow field in the vicinity of the tube wall in turbulent pipe flow consists in part of a transient elongational flow (Seyer and Metzner, 1969), suppression of turbulence production and dissipation may occur. In our earlier VI studies, we noted that the fluid motion just below the surface dimple or depression also appeared to possess a stretching or extensional character, thus suggesting one possible explanation for the correlation between VI and drag reduction. However, for a thorough mathematical investigation of VI, it is clear that a detailed analysis of the velocity field is required.

## EXPERIMENTAL

Velocity profile measurements were made in a cylindrical Plexiglas tank, 44.5 cm in diameter and 66.0 cm high. The liquid level was maintained at 54.5 cm relative to the tank bottom by manually controlling the rate of fluid entering. Fluid entered the tank through two vertical distributor tubes, placed 180 deg. relative to one another along the tank wall. The orifice holes in the distributor tubes were directed tangentially to the wall, so that a swirling motion was imparted to the fluid in the tank.

In order to better compare the velocity profile rearrangements resulting from polymer addition, a smaller exit orifice (0.516 cm I.D.) in the tank was used than with our previous VI experiments (1.27 cm I.D.). This eliminated air core formation with water, and thus superficially the appearance of the surface of the polymer solution was similar to that of water, consisting of a slight depression or dimple. The flow rate was 50 cm$^3$/s in all instances.

Measurements of the velocity profile were made by using a technique similar to that of Turner (1966). Small neutrally buoyant particles of Pliolite (Goodyear Company) were added to the liquid. These particles reflect light and show up as streaks on the photographic film. The tank was illuminated by using a Kodak slide projector, and a slit shaped slide allowed us to focus the beam on a narrow section of fluid. The light beam was interrupted by a chopper wheel, such that the duration of each burst was 0.0247 s. By using this technique, the axial and tangential components of the velocity vector could readily be obtained. Tangential profiles were highly reproducible (± 2-3%); the axial velocity measurements tended to be less precise, owing to oscillations, but were usually reproducible to within 0.25 cm/s. The polymer solution consisted of 3 p.p.m. (by weight) Separan AP 273, a partially hydrolyzed polyacrylamide made by Dow, in deionized water.

## RESULTS AND DISCUSSION

### Tangential Velocity

Tangential velocity profile measurements for water and polymer solution at a depth of 20 cm below the liquid surface are presented in Figure 1. The presence of the

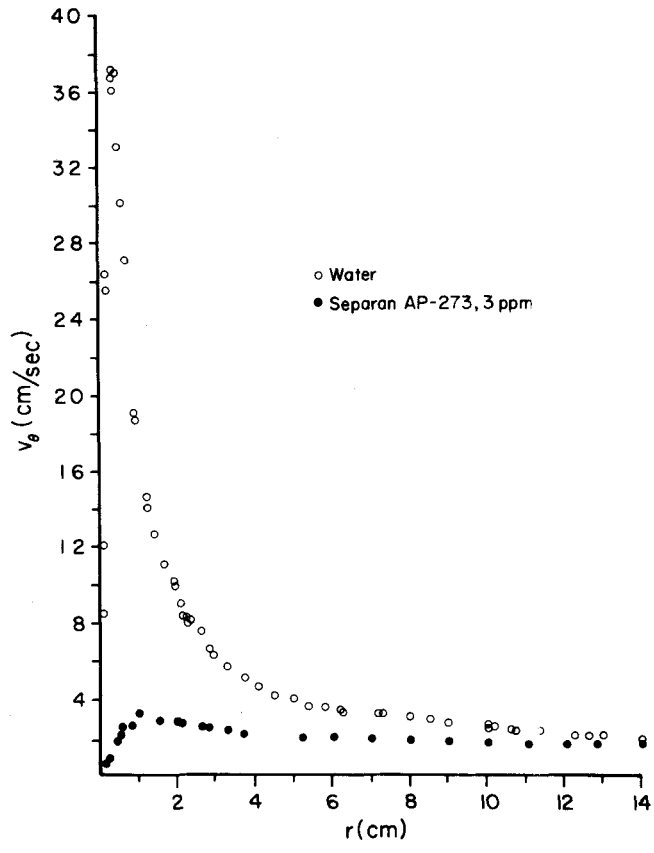


**Fig. 1. Measured tangential velocity profiles for water and polymer solution, in an axial plane 20 cm below the level of the liquid surface at the tank center line.**

polymer leads to a dramatic decrease in tangential velocity, particularly in the core region of the flow field. The resulting centrifugal force field tends to suppress vortex or air core formation, as may be seen from the following analysis.

We choose the origin of our coordinate system at the center of small depression (dimple) on the liquid surface. In cylindrical coordinates, with the $z$ axis pointing downward, the equations of motion (Bird, Stewart, and Lightfoot, 1960) reduce to

$$-\frac{\rho v_\theta^2}{r} = -\frac{\partial \pi_{rr}}{\partial r} + \frac{\pi_{\theta\theta} - \pi_{rr}}{r} \tag{1}$$

$$v_r \frac{\partial v_\theta}{\partial r} + \frac{v_r v_\theta}{r} = -\frac{1}{\rho r^2}\frac{\partial}{\partial r}(r^2 \pi_{r\theta}) \tag{2}$$

$$\frac{\partial \pi_{zz}}{\partial z} = \rho g \tag{3}$$

where $\pi$ is the total stress. To obtain Equations (1) to (3), we have used the experimentally determined velocity profile measurements along with the continuity equation (Bird, Stewart, and Lightfoot, 1960) to show that

$$v_r \frac{\partial v_r}{\partial r} << \frac{v_\theta^2}{r} \tag{4}$$

and

$$v_z \frac{\partial v_z}{\partial z} << g \tag{5}$$

$v_\theta$ was found to be independent of $z$ in the bulk of the tank, and $v_z$ increased linearly with increasing $z$ except in the region very close to the tank bottom, where $v_z$ began to increase very rapidly (Figure 3). Near the vortex core, where $dv_r/dr$ is small, the following approximations are

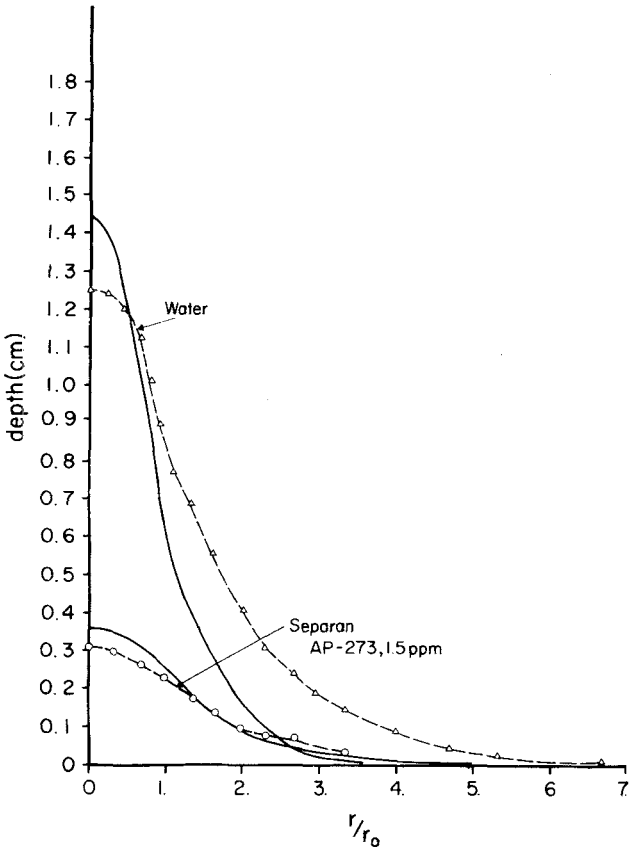


Fig. 2. Comparison of predicted (solid lines) and measured (dashed lines) surface shapes for water and polymer solution. Depth refers to distance below level of the liquid surface at tank wall. $r_o = 0.75$ cm in both cases.

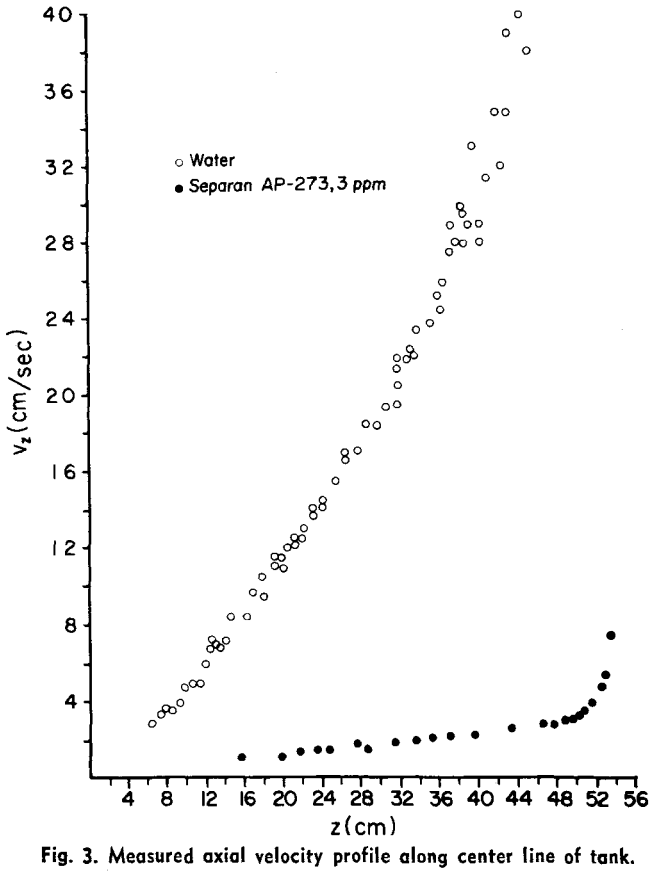


Fig. 3. Measured axial velocity profile along center line of tank.

reasonable:

$$\pi_{rr} = p \tag{6}$$

and

$$\pi_{zz} = p + \mu_e \frac{\partial v_z}{\partial z} \tag{7}$$

where $\mu_e = \mu_e\left(\frac{\partial v_z}{\partial z}\right)$ only. In the case of the polymer solution, the extensional viscosity $\mu_e$ may be many times larger than the shear viscosity (Balakrishnan and Gordon, 1975*b*). From Equations (1), (3), (6), and (7) and the noted linear dependence of $v_z$ on $z$, the following expression for the pressure $p$ may be obtained:

$$p = \rho g z + \int_0^r \frac{\rho v_\theta^2}{r}\, dr \tag{8}$$

The locus of the free surface is then

$$z_s = -\frac{1}{g}\int_0^r \frac{v_\theta^2}{r}\, dr \tag{9}$$

Calculated shapes for water and polymer solution indicate that reduction of the tangential velocity with polymer leads to a smaller surface depression or dimple and presumably less tendency to form an air core. Experimentally, almost complete absence of any depression was observed at a polymer concentration of 3 w.p.p.m. Lowering the concentration to 1.5 w.p.p.m. increased $v_\theta$ and led to a noticeable dimple. In Figure 2, the measured surface shapes for polymer (at 1.5 w.p.p.m.) and water are compared with the theoretical predictions. Here, $r_o$ is the radius of the solid core, within which $v_\theta$ is linear in $r$. Equation (9) is in rough agreement with the measured profile for water and in fairly close agreement in the case of the polymer solution. This is reasonable in view of the fact that the assumptions involved in the derivation of the expression for $z_s$, such as Equations (4) and (5), hold much more closely for the polymer solution.

### Axial Velocity

Figure 3 illustrates the large reduction in axial velocity which occurs in the presence of the polymer. This finding may be used to predict the observed decrease in tangential velocity in the following manner. Starting with the $\theta$ component of the equation of motion, we write

$$\pi_{r\theta} = -\mu_s \frac{\partial v_\theta}{\partial r} \tag{10}$$

When we introduce the definitions

$\Gamma = r v_\theta$ circulation

$\eta = r^2/r_o^2$ dimensionless radius

Equation (2) reduces to

$$2\eta \frac{d^2\Gamma}{d\eta^2} - \frac{\rho r v_r}{\mu_s}\frac{d\Gamma}{d\eta} = 0 \tag{11}$$

From the continuity equation, $v_r$ is given by

$$v_r = -\frac{r_o^2}{2r}\int_0^\eta \frac{\partial v_z}{\partial z}\, d\eta \tag{12}$$

where $\partial v_z/\partial z$ is a function of $\eta$. Combining Equations (11) and (12), integrating, and using the boundary condition that

$$\Gamma(\eta \to \infty) = \Gamma_\infty, \quad \text{inlet circulation}$$

we get

$$\frac{\Gamma}{\Gamma_\infty} = \frac{\int_0^\eta \exp\left[-\int_0^s \frac{\rho r_o^2}{4\mu_s t}\left(\int_0^t \frac{\partial v_z}{\partial z}\,dt'\right)dt\right]ds}{\int_0^\infty \exp\left[-\int_0^s \frac{\rho r_o^2}{4\mu_s t}\left(\int_0^t \frac{\partial v_z}{\partial z}\,dt'\right)dt\right]ds} \tag{13}$$

where $s$, $t$, and $t'$ are dummy integration variables. [Note that $\partial v_z/\partial z = \partial v_z/\partial z(t')$.] From estimated values for $\Gamma_\infty$, from the circulation at the tank wall, and from experimental measurements of $\partial v_z/\partial z$ vs. $\eta$, Equation (13) was found to closely approximate the measured tangential velocity profiles. Inspection of Equation (13) also indicates directly that reduction of the axial velocity gradient in the core region implies a corresponding reduction in tangential velocity, indicative of vortex inhibition. The precise explanation for the very small axial gradient in the polymer solution is still obscure; it may be related to the large values of $\mu_e$ for this system. This is currently under study.


## ACKNOWLEDGMENT

The authors gratefully acknowledge support for this work under NSF grant ENG75-09350. Helpful comments were provided by Professor J. L. Zakin.


## NOTATION

$g$ = gravitational acceleration
$p$ = isotropic pressure
$r$ = radial coordinate
$r_o$ = radius of solid core, for which $v_\theta$ is linear in $r$
$v_i$ = $i^{\text{th}}$ component of velocity vector
$z$ = axial coordinate (points toward tank bottom)
$z_s$ = axial coordinate of free surface (a negative quantity)

### Greek Letters

$\Gamma$ = circulation ($rv_\theta$)
$\Gamma_\infty$ = circulation at $r = \infty$ (tank wall)
$\eta$ = dimensionless radial coordinate $(r/r_o)^2$
$\mu_e$ = extensional viscosity defined by Equation (7)
$\mu_s$ = shear viscosity defined by Equation (10)
$\pi_{ij}$ = $i,j^{\text{th}}$ component of total stress tensor
$\rho$ = density

## LITERATURE CITED


Balakrishnan, C., and R. J. Gordon, "New Viscoelastic Phenomenon and Turbulent Drag Reduction," *Nature Phys. Sci.*, **231**, 25 (1971).

———, "Influence of Molecular Conformation and Intermolecular Interactions on Turbulent Drag Reduction," *J. Appl. Polymer Sci.*, **19**, 909 (1975*a*).

———, "Extensional Viscosity and Recoil in Highly Dilute Polymer Solutions," *AIChE J.*, **21**, 6 (1975*b*).

Bird, R. B., W. E. Stewart, and E. N. Lightfoot, *Transport Phenoma*, J. Wiley, New York (1960).

Everage, A. E. Jr., and R. J. Gordon, "On the Stretching of Dilute Polymer Solutions," *AIChE J.*, **17**, 5 (1971).

Gordon, R. J., and C. Balakrishnan, "Vortex Inhibition: A New Viscoelastic Effect with Importance in Drag Reduction and Polymer Characterization," *J. Appl. Polymer. Sci.*, **16**, 1629 (1972).

Little, R. C., R. J. Hansen, D. L. Hunston, O. Kim, R. L. Patterson, and R. Y. Ting, "The Drag Reduction Phenomenon. Observed Characteristics, Improved Agents, and Proposed Mechanisms," *Ind. Eng. Chem. Fundamentals*, **14**, 4 (1975).

Metzner, A. B., and A. P. Metzner, "Stress Levels in Rapid Extensional Flows of Polymeric Fluids," *Rheol. Acta.*, **9**, 2 (1970).

Paterson, R. W., and F. H. Abernathy, "Turbulent Flow Drag Reduction and Degradation with Dilute Polymer Solutions," *J. Fluid Mech.*, **43**, 4 (1970).

Seyer, F. A., and A. B. Metzner, "Turbulence Phenomena in Drag Reducing Systems," *AIChE J.*, **15**, 3 (1969).

Turner, J. S., "The Constraints Imposed on Tornado-Like Vortices by the Top and Bottom Boundary Conditions," *J. Fluid Mech.*, **25**, 377 (1966).



*Manuscript received February 17, 1976; revision received May 25, and accepted May 26, 1976.*


# An Empirical Method for Evaluating Critical Molar Volumes


**ALESSANDRO VETERE**

**Laboratori Ricerche Chimica Industriale**
**Snamprogetti, San Donato Milanese**
**Italy**


The experimental determination of critical molar volumes has proven to be an unusually difficult problem. As a consequence, experimental values of $V_c$ are known for only a relatively few compounds and with an error which is not always negligible. Furthermore, the critical properties of some compounds must be estimated because their instability at the critical point prevents the experimental determination. On the other hand, even if a great amount of effort has been devoted to the development of empirical methods for estimating this parameter, it is generally admitted that correlation methods for $V_c$ are still less satisfactory than correlations for other critical properties (Reid and Sherwood, 1966).

Lacking experimental data, and with the unreliability of the prevision methods, we have, until now, been prevented from using $V_c$ for estimating thermodynamic and volumetric properties of fluids by the theorem of corresponding states (Pitzer et al., 1955).

The purpose of this work was to examine the best empirical methods for critical volumes and to develop a more precise correlation based on additive group contributions to estimate $V_c$ from the knowledge of the chemical structure and molecular weight.

## METHOD FOR $V_c$ EVALUATION

Empirical correlations for evaluating critical volumes have been reviewed by Reid and Sherwood (1966)), Kudchadker et al. (1968*a*), and Spencer and Daubert (1973). Only recent developments or methods of wide applica-